Nano Energy 100 (2022) 107443

Contents lists available at ScienceDirect

Nano Energy

journal homepage: www.elsevier.com/locate/nanoen

A droplet-based electricity generator for large-scale raindrop energy harvesting☆

Zong Li [a,f], Daiming Yang [b], Zhonghao Zhang [a,g], Shiquan Lin [c,d], Bin Cao [a,*], Liming Wang [a], Zhong Lin Wang [c,e,**], Fanghui Yin [a]

[a] Tsinghua Shenzhen International Graduate School, Tsinghua University Shenzhen, 518055 Guangdong, PR China
[b] Department of Construction & Environment, Shenzhen Polytechnic, Shenzhen 518055, Guangdong, PR China
[c] Beijing Institute of Nanoenergy and Nanosystems, Chinese Academy of Sciences, Beijing 100083, PR China
[d] School of Nano Science and Technology, University of Chinese Academy of Sciences, Beijing 100049, PR China
[e] School of Materials Science and Engineering, Georgia Institute of Technology, Atlanta, GA, 30332-0245, USA
[f] State Grid Qingdao Power Supply Company, State Grid, Qingdao 266002, Shandong, PR China
[g] China Electric Power Research Institute, Haidian District, Beijing 100192, PR China

ARTICLE INFO

Keywords:
Droplet-based electricity generator
Large-scale raindrop energy harvesting
Self-capacitance effect
Simple open structure

ABSTRACT

Droplet-based electricity generator (DEG) has been demonstrated as efficient method to harvest energy from the natural environment. However, the complex structure and low output power density are still two barriers to wide applications. To this end, by making full use of the self-capacitance effect of the upper electrode, a droplet-based electricity generator with a simple open structure (SCE-DEG) was proposed in this paper. The working principle of SCE-DEG and the effects of electrode geometry and droplet parameters (volume, conductivity, and dropping frequency) on its output voltage were analyzed. Compared with the DEG, the upper electrode of SCE-DEG does not need to connect to the lower electrode and the ultra-high instantaneous peak output power (765 W/m^2) can still be achieved by self-capacitance effect of the upper electrode. This research provides a reference for the large-scale raindrop energy harvesting.

1. Introduction

Affected by the clouds and rainfalls, the power generation of solar panels in some humidity areas are is not efficiently. Because of the abundant renewable energy in the rains, collecting the energy from them is of great significance to realize "carbon zero" for the whole world [1–5]. The traditional method of harvesting the rain energy is collecting raindrops into the reservoirs and then generating electricity through a hydro electromagnetic generator. However, due to the many shortcomings, namely, high-cost of construction, difficulty to realize distributed energy collection and unsuitable for low-frequency energy collection, it is difficult to be popularized on a large scale [6–9].

As a new generation of energy harvesting technology, triboelectric nanogenerator(TENG) has attracted global researchers, because of its simple structure, low cost material fabrication, good low-frequency characteristics and easy energy harvesting from the distributed system [10–19]. The droplet-based TENG started in 2014 [20], Zhonglin Wang and his collaborators studied the principle of contact electrification and electrostatic induction between water droplets and insulating materials and realized the energy harvesting with TENG from rain, but the output power was just 0.02 W/m^2 [21].

To improve the output power of droplet-based TENG, Wang and others proposed a droplet-based electricity generator (DEG) with a "Transistor-like" structure and improved the output of instantaneous power greatly to 50.1 W/m^2 in 2020 [22,23]. Since then, DEG was developed and researchers realized the energy harvesting from ocean waves [24–27], rain [28–36] and so on [37–40].

DEG proposed in [22] has ultra-high instantaneous peak power

☆ Prof Zhong Lin Wang, an author on this paper, is the Editor-in-Chief of Nano Energy, but he had no involvement in the peer review process used to assess this work submitted to Nano Energy. This paper was assessed, and the corresponding peer review managed by Professor Chenguo Hu, also an Associate Editor in Nano Energy.

* Corresponding author.
** Corresponding author at: Beijing Institute of Nanoenergy and Nanosystems, Chinese Academy of Sciences, Beijing 100083, PR China.
E-mail addresses: cao.bin@sz.tsinghua.edu.cn (B. Cao), zhong.wang@mse.gatech.edu (Z.L. Wang).

https://doi.org/10.1016/j.nanoen.2022.107443
Received 2 April 2022; Received in revised form 28 May 2022; Accepted 30 May 2022
Available online 6 June 2022

output and it is a huge advance in droplet-based electrical generators. However, it is difficult to continuously provide energy for the electrical equipment by a single or several DEGs. When harvesting large-scale raindrop energy in sloping buildings such as sheds, a simple method is to connect all DEGs in parallel to supply power to the load (like a bulb). With reference to the cell structure of a solar panel and by making full use of the self-capacitance effect of the upper electrode, this paper proposed a droplet-based electricity generator (SCE-DEG) with a simple open structure.

SCE-DEG is mainly composed of the upper electrode, PTFE film, lower electrode and load (Fig. 1b). Compared with the DEG, the upper electrode does not need to connect to the lower electrode and the ultra-high instantaneous output power can be achieved by the self-capacitance effect of the upper electrode, which makes its structure much simple and more convenient for large-scale popularization.

2. Results and discussions

2.1. High-performance of the SCE-DEG

The simple structure of self-capacitance of electrode droplet-based electricity generator can be easily installed on buildings with inclination such as sheds and houses and realize the collection of raindrop energy (Fig. 1a). Fig. 1bl and Supplementary Fig.S1aI show the structure of SCE-DEG. It is mainly composed of three components: upper electrode, insulating layer (PTFE dielectric film) and lower electrode, but the upper electrode and the lower electrode do not need to be directly connected. For comparison, we also made control device (Fig. 1bII and Supplementary Fig. S1aII) and DEG (Supplementary Fig. S1aIII).

When a 60 μL tap water droplet dripping from 20 cm height with 10 Hz frequency, the measured output voltage (Oscilloscope probe impedance 100 MΩ) of SCE-DEG is 250 V, which is nearly 35 times higher than that of traditional TENG (Fig. 1c). Compared with DEG, its output voltage remains the same (Supplementary Fig. S1aIII), but no physical connection between the upper and lower electrodes, which is convenient for large-scale energy harvesting. When a 61 μL tap water droplet falls from 20 cm height with 2.85 cm^2 maximum spreading area, the instantaneous peak output power of SCE-DEG ($P = V^2/R$) with 200 kΩ load impedance is 60 mW (Supplementary Fig. S2a). When a 61 μL salt solution droplet falls from 20 cm height, the instantaneous peak output power of SCE-DEG with 10 kΩ load impedance is 212 mW (Supplementary Fig. S2b) and the instantaneous peak output power of SCE-DEG is 765 W/m^2, which is much higher than the previous researches [20–22,24,34,38,40], as shown in Fig. 1d.

2.2. The working principle of the SCE-DEG

To clarify the working principle of SCE-DEG, the power generation process of SCE-DEG are divided into four stages, as shown in Fig. 2a. In the first stage, the dripped water droplet collides with the PTFE film, making the droplet and PTFE surface positively and negatively charged respectively. Then, when the water droplet detaches from the PTFE film, the PTFE film and the lower electrode carry the same amount charges but with different polarity. Although the charge generated by each droplet is small after hundreds of droplets colliding, PTFE's surface potential is high due to charge accumulation, and when the charges generated by the droplets and the charge dissipating on the PTFE film reach a balance, the charge on the PTFE dielectric film reaches a saturation state. Once the PTFE surface is charged by droplets, when the next droplet collides with the PTFE film (Fig. 2aI), the water droplet is polarized and the positive charge in the water droplet approaches the PTFE surface, while the negative charge moves towards the interface between the water droplet and air (Fig. 2aII).

Then, the water droplet contacts the upper electrode (Fig. 2aIII), the bound negative charges in the droplet and the bound positive charges in the upper electrode move and form an electric double layer. As under steady-state conditions, the surface potential of the upper electrode and the droplet should be equal, and the bound negative charge in the water and some positive charges induced by the upper electrode flow to both sides of the electric double layer, resulting in the weakening of the attraction of the positive charge of the lower electrode. As part of the positive charge of the lower electrode flows into the earth, and the current generates and flows through the load. Since the contact area between the water and the upper electrode increases first and then

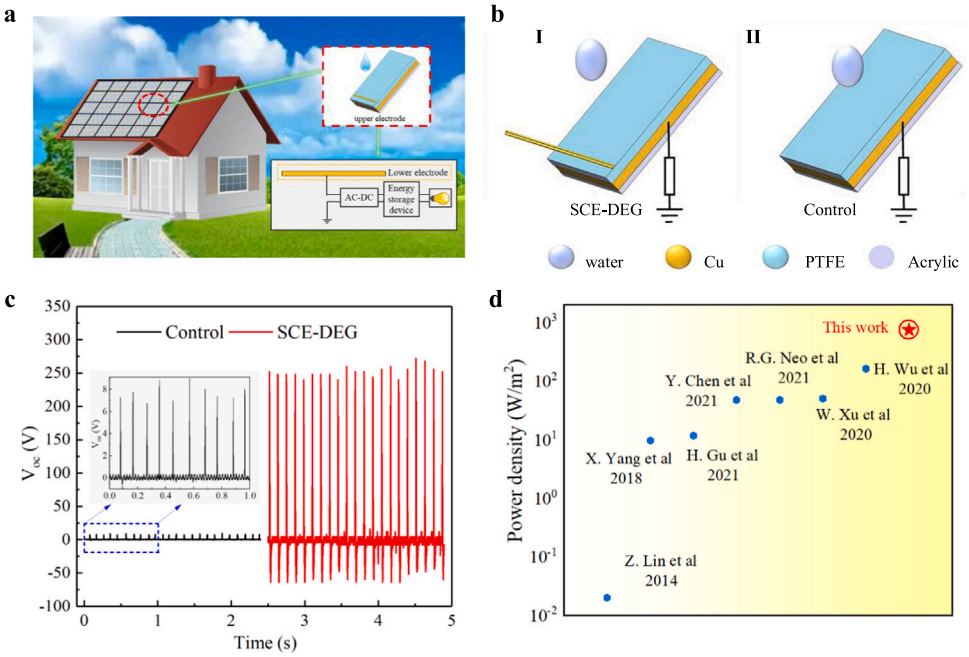

Fig. 1. Design and high performance of the SCE-DEG. (a)Application of SCE-DEG on the building's roofs. (bI) SCE-DEG and (bII) the control device of traditional droplet-based TENG. (c) output voltage of SCE-DEG and the control device. (load resistance R_L of 100 MΩ) (d) Comparison of the instantaneous power density obtained in this work with other reports.

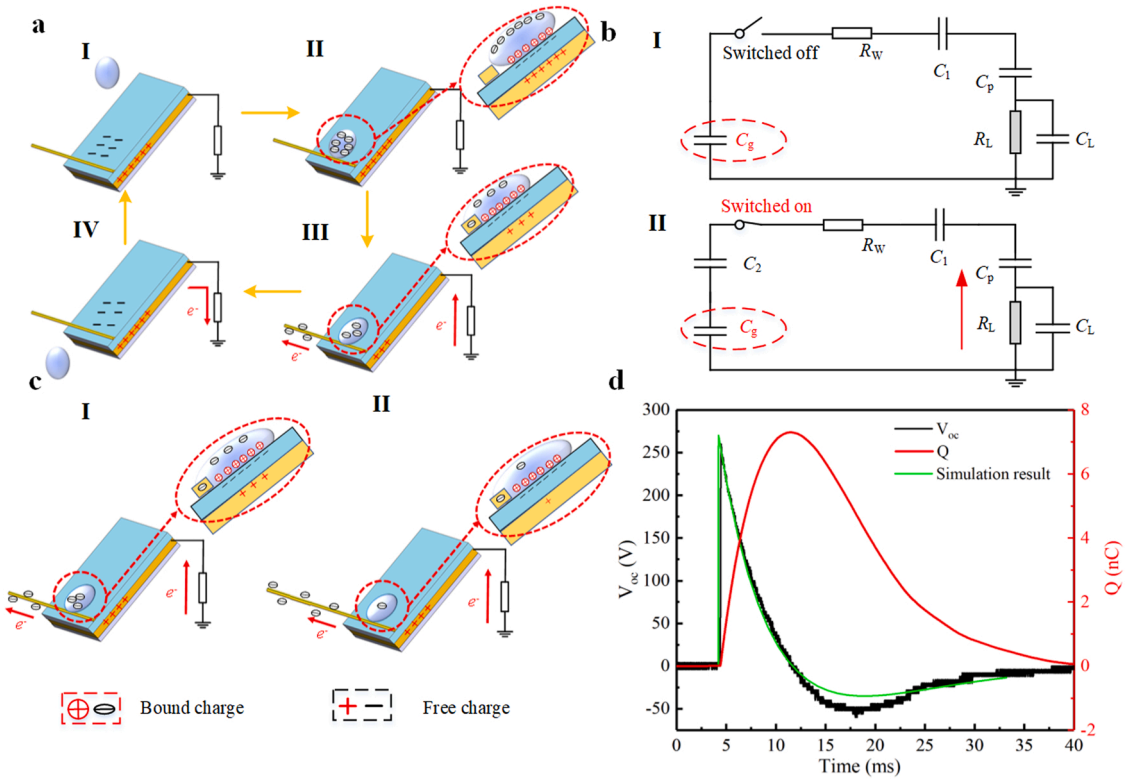

Fig. 2. Working principle of the SCE-DEG. (a) the working principle of the SCE-DEG. (b) equivalent circuit (I.) In the switched-off mode (II.) In the switched-on mode, (c) effect of upper electrode length. (d) Change of output voltage and charge by a single water droplet.

decreases, and the electric double-layer capacitance between the water droplets and the upper electrode also change with the same trend, the open-circuit voltage is first positive and then negative, which forms an alternating voltage.

During the charge transfer process, since water is a strong polar electrolyte, the charge density is proportional to $exp(-\sigma t/(\varepsilon_0\varepsilon_2))$ (Supplementary Note.S1), and the time constant $\varepsilon_0\varepsilon_2/\sigma$ is the polarization relaxation time. For a distilled water droplet with a conductivity of 0.5 μS/cm, the polarization release time is 1.6×10^{-5} s. Therefore, the change of the output voltage is mainly affected by the change rate of the double capacitance, which is determined by the contact area between the water droplet and the upper electrode. In this paper, the duration of positive voltage and negative voltage caused by each droplet is about 7 ms and 20 ms, which is related to the contact time of the water droplet and the electrode in the experiment.

On the other hand, the larger the geometric size of the upper electrode is, when the surface potential of water droplets and upper electrode reaches equilibrium, the more bound charges on the upper electrode's surface, and the higher the output voltage with the same load impendence(Fig. 2c). Similarly, the more the accumulating charge on the PTFE surface is, the higher output voltage could be obtained.

The equivalent circuit of the SCE-DEG is shown in Fig. 2b. When the water droplet is on the PTFE surface without contacting the upper electrode is shown in Fig. 2bI, where C_P represents the equivalent capacitance between the PTFE film and the lower electrode, C_1 represents the double layer capacitance between the water droplet and the PTFE film, R_W is the equivalent resistance of the water droplet, and C_g represents the upper electrode's self-capacitance, that is, the equivalent capacitance between the upper electrode and the ground (reference point for electric potential). When the water droplets expand on the PTFE surface and do not contact the upper electrode, the whole circuit is equivalent to an open circuit state.

When the droplet contacts the upper electrode, the switch is closed and the new formed electric double layer (the water droplet and the upper electrode) can be equivalent to a new capacitance C_2. The initial charges on the C_P are redistributed on the capacitance C_P, C_1, C_2 and C_g. It is obviously that C_g plays a important role in the whole closed circuit and with a higher value, the output voltage is higher with the same load impendence (Supplementary Note.S2). During charge transfer process, the current will flow though the load and produce an alternating voltage.

Fig. 2d shows the change of output voltage and charge transfer during the power generation cycle of a single water droplet. The transferred charge, which could indicate the charge flowing through the load, was calculated be the measured output voltage with load resistor. When the water drop contacts the upper electrode (at the time t_{on}), the voltage increase instantaneously and the charge transfer starts. Then, with the expansion of water droplets on the PTFE surface, the open-circuit decreases gradually and after several microseconds, the charge begins to flow in the opposite direction, which makes the load voltage negative. Finally, when the water droplet completely separates from the upper electrode (at the time t_{off}), the charge transfer end and the voltage become zero, which could be verified by the circuit simulation, as shown in green lines in Fig. 2d.

2.3. *Effects of electrode geometry*

The effects of the lengths, radius and connection mode of the upper electrode on the output power of SCE-DEG are shown in Fig. 3. With the increase of the upper electrode length, the output voltage of SCE-DEG increases gradually. Fig. 3a shows the output voltage of SCE-DEG with the upper electrode of 0.31 mm radius but different lengths. The output voltage with 40 cm upper electrode is 88 V, which is nearly twice voltage (45 V) with 20 cm length and nearly four times the voltage (23 V) with 10 cm length. However, with the further increase of the upper electrode length, the output voltage reaches saturated (when the length of the upper electrode is 10 m, the open-circuit voltage is 225 V).

To analyze the effect of electrode size on output voltage, we also

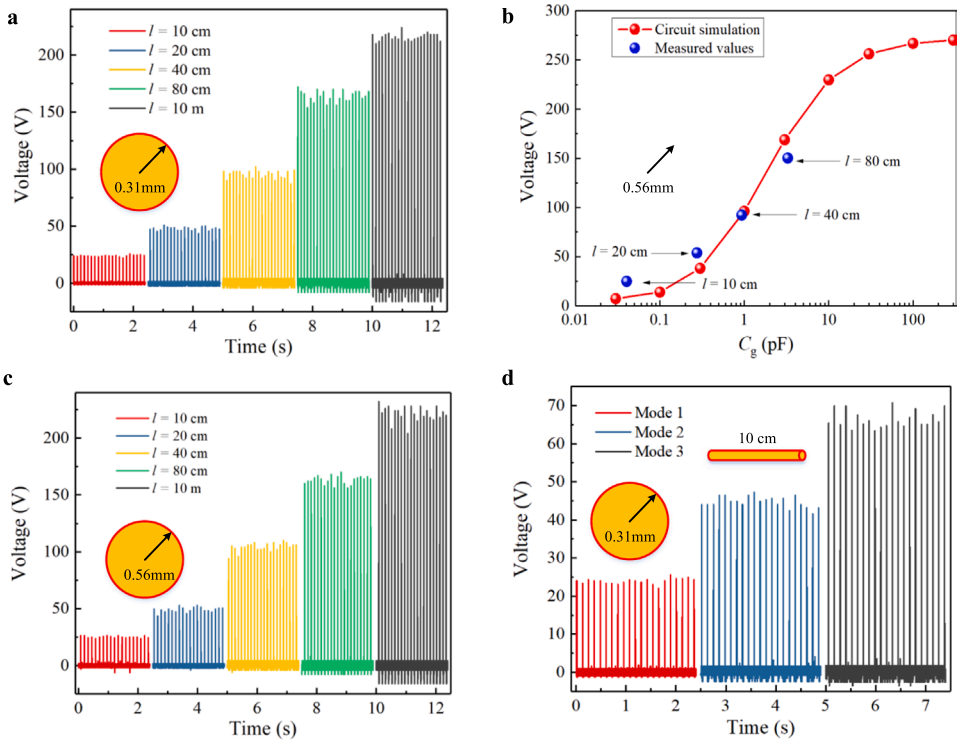

Fig. 3. Effects of Electrode geometry (h=20 cm, 61 μL, f=10 Hz, R_L = 20 MΩ). (a) the output voltage with electrode different length(R=0.31 mm). (b) the relationship between output voltage, upper electrode capacitance and length. (c) the output voltage with electrode different length(R=0. 56 mm). (d) SCE-DEG output voltage with different upper electrode arrangements. Three arrangements and water droplet collision area are depicted in Supplementary Fig. S3.

calculated the output voltage U_L of SCE-DEG with different self-capacitance C_g by circuit simulation (Supplementary Note. S2), as well as the C_g value with different electrode lengths by the finite element calculation (Supplementary Note. S3). The results are collectively shown in Fig. 3b. With the increase of self-capacitance, the output voltage reaches saturation.

Fig. 3c shown the output voltage of SCE-DEG with 0.56 mm electrode radius and the voltage is nearly the same as that with 0.31 mm upper electrode radius. the radius have no obvious effect on the output voltage. Fig. 3d shows the SCE-DEG output voltage with different upper electrode arrangements. The output voltage of SCE-DEG with two 10 cm connected in mode 2 is nearly the same as that with a single 20 cm upper

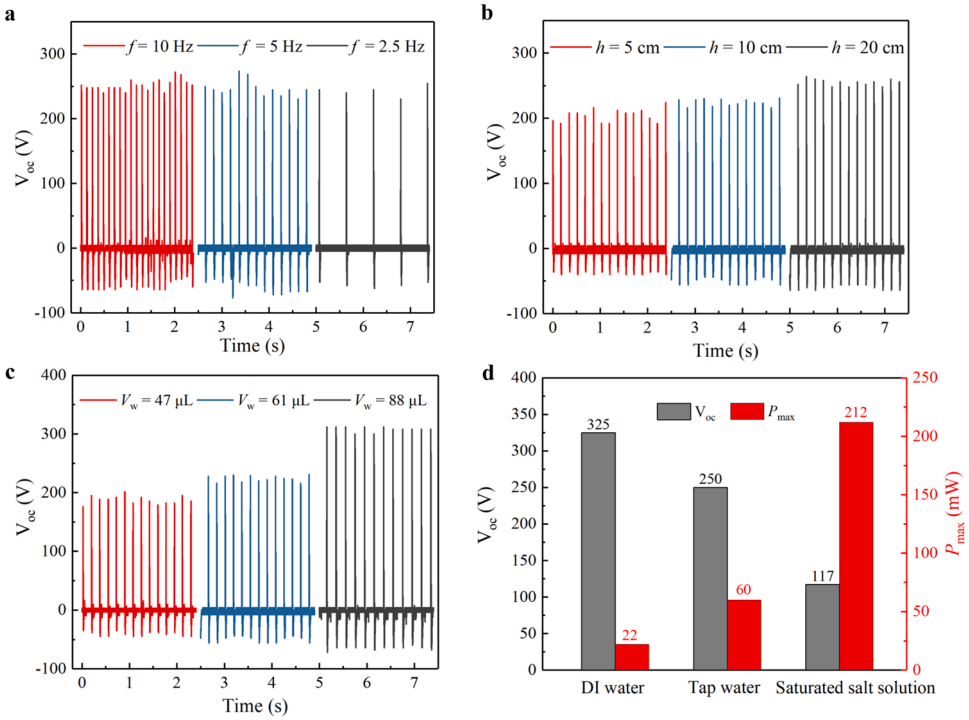

Fig. 4. Effect of water droplets parameters on the output voltage. (a) frequency (b) height (c) droplet volume (d) water conductivity.

electrode. It indicates that SCE-DEG is easy to expand and has application prospects in large-scale energy harvesting.

2.4. Effects of water droplet parameters

Effects of water dropping frequency (2.5 Hz, 5 Hz and 10 Hz) and water conductivity on SCE-DEG's performance were also studied. As the dissipation time of charge on the PTFE's surface decreases with the dropping frequency, the instantaneous output voltage of SCE-DEG increases slightly with the water dropping frequencies, as shown in Fig. 4a. It also should be noted that, as the superhydrophobic surface makes the water droplets easy to slide off without a continuous water film, when the water dropping frequency is higher than 100 Hz, the use of superhydrophobic materials can effectively maintain the generator's output efficiency [33].

Fig. 4b and Fig. 4c shows the output voltage of water droplets at different initial heights and generated by the droplets of different sizes. When the height increases from 5 cm to 20 cm, the output voltage increases less than 25%, which is related to the spreading area on PTFE when water droplets collide (Supplementary Note.S2).

The effect of water conductivity on output voltage and output power was also studied, as shown in Fig. 4d and Supplementary Fig.S2, when the water conductivity is low, SCE-DEG's output voltage is high, but the maximum output power is low. The open-circuit voltage of SCE-DEG generated by the deionized water (conductivity of 4 μS/cm) is the highest (325 V), but the instantaneous peak output power is only 22 mW with 2 MΩ load impedance, while the open-circuit voltage of SCE-DEG generated by the saturated salt solution (conductivity 4600 μS/cm) is 117 V, but the instantaneous peak output power reaches 212 mW with 10 kΩ load impedance.

The effect of water conductivity on SCE-DEG's output voltage is determined by multiple factors. On the one hand, the higher ion concentration in salt solution reduces the charge accumulated on the PTFE surface and lead to the lower output voltage of the SCE-DEG. On the other hand, the conductivity of water droplets affects the SCE-DEG's equivalent impedance R_w. Due to the high resistivity R_w with the deionized water, the output power of the SCE-DEG is low, which could be verified by the load maximum instantaneous peak power equation as follows:

$$P_{max} = \frac{V_{oc}^2}{4R_w} \quad (1)$$

Where, P_{max} is the maximum instantaneous peak output power, R_w is the equivalent impedance of SCE-DEG. For the saturated salt solution, Its R_w is much less than that of tap water, but the V_{oc} is half of it. Therefore, the SCE-DEG can get such high output power (765 W/m^2).

2.5. Application

The applications of SCE-DEG on the charging of capacitors, calculators and LEDs were studied. Fig. 5a shows it takes about 100 s, 20 s and 4 s to charge the 4.7 μF, 1 μF and 0.47 μF capacitors to 2 V by the SCE-DEG with the tap water droplets (h= 20 cm, f = 10 Hz, V_w = 61 μL). The capacitor voltage is linear to the charging time, which means the charge transferred by each droplet is almost unchanged. Fig. 5b shows the charging characteristics of the capacitors with different dripping frequencies (h= 20 cm, C_s = 0.47μF. Tap water). When the dripping frequency is high, the capacitor voltage increases almost linearly with time and when the 4.7 μF capacitor's voltage was charged to 2 V by SCE-DEG, it could power on the electronic calculator (Fig. 5c); When SCE-DEG was connected to LEDs directly, it could light up more 100 commercial LEDs (specifications in Supplementary Note.S4) with one water droplet (tap water, h=20 cm, f=10 Hz), which showed an ultra-high-output performance (Supplementary movie 1).

Supplementary material related to this article can be found online at doi:10.1016/j.nanoen.2022.107443.

3. Conclusion

In summary, this paper proposed a droplet-based SCE-DEG with a simple structure. Based on the self-capacitance of the upper electrode, the SCE-DEG could effectively harvest raindrop energy. The test results

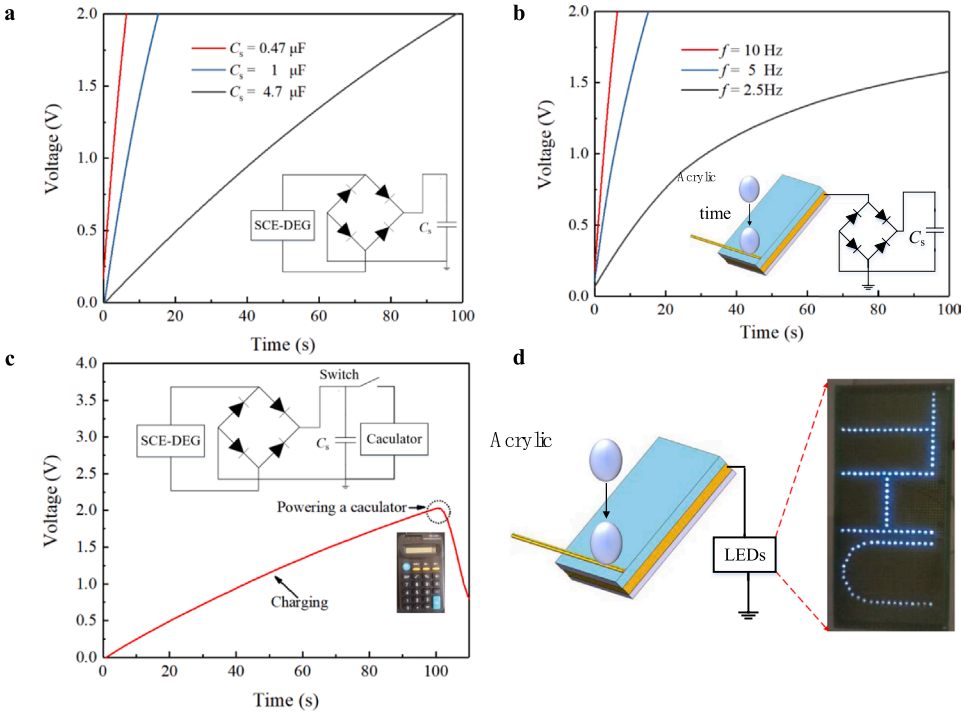

Fig. 5. Applications of SCE-DEG on the capacitors, calculators and LEDs (a) the charging curve of different capacitors by SCE-DEG (b) with different water dripping frequencies (c) energizing the commercial calculator (d) light up 100 small commercial LED lights.

showed it could produce 212 mW output power by a 61 μL water droplet and can direct light up 100 commercial LEDs. As with a simple structure, high output power and good low-frequency energy harvesting characteristics, SCE-DEG might provide a practical scheme for the large-scale popularization and application of droplet-based TENG.

4. Experimental section

4.1. The fabrication of the SCE-DEG

As shown in Fig. 1b, after cleaning the 40 * 40 * 0.02 mm^3 PTFE film with acetone and ethanol, the lower electrode (40 *40 *0.05 mm^3 copper tape) was pasted on its back. Then, fix the upper electrode (a copper rod with a specific length or radius) on the PTFE's upper surface. Finally, paste the lower electrode on the supporting material (40 *40 *5 mm^3 acrylic board). All materials used are available in the market.

4.2. Characterization and electrical measurement of the SCE-DEG

In the experiment, the atmospheric temperature and relative humidity was kept at 50 ± 5% and 20.0 ± 5 ℃ respectively. The water droplet was generated by the commercial infusion sets. The output voltage of the SCE-DEG was measured by a digital oscilloscope (RIGOL, DS1102) with a highly attenuated voltage probe (100 MΩ).

CRediT authorship contribution statement

Zong Li: Conceptualization, Methodology, Investigation, Writing - Original Draft, Writing - Review & Editing. **Daiming Yang:** Software, Writing - Review & Editing, Validation. **Zhonghao Zhang:** Software, Validation. **Shiquan Lin:** Writing - Review & Editing, Data Curation. **Bin Cao:** Methodology, Supervision, Funding acquisition, Validation, Writing - Review & Editing. Resources **Liming Wang:** Project administration, Funding acquisition, Resources. **Zhonglin Wang:** Supervision, Writing - Review & Editing, Data Curation. **Fanghui Yin:** Resources, Writing - Review & Editing.

Declaration of Competing Interest

The authors declare that they have no known competing financial interests or personal relationships that could have appeared to influence the work reported in this paper.

Acknowledgments

This work was supported in part by the National Natural Science Foundation of China (NSFC) under Grant No. 52007095 and in part by NSFC under Grant No. 51977118.

Appendix A. Supporting information

Supplementary data associated with this article can be found in the online version at doi:10.1016/j.nanoen.2022.107443.

References

[1] S. Lin, X. Chen, Z. Wang, Contact electrification at the liquid–solid interface, Chem. Rev. 122 (2022) 5209–5232.
[2] Y. Lin, Y. Liu, K. Wu, L. Wang, L. Ding, Dynamic electrical conductivity induced by isothermal crystallization in aluminum hydroxide filled silicone rubber, Appl. Phys. Lett. 119 (2021), 152902.
[3] S. Lin, L. Xu, A.C. Wang, Z.L. Wang, Quantifying electron-transfer in liquid-solid contact electrification and the formation of electric double-layer, Nat. Commun. 11 (2022) 399.
[4] Z. Cheng, Z. Hou, Y. Wang, M. Guo, K. Wu, J. Li, Y. Lin, Steadily decreasing power loss of a double Schottky barrier originating from the dynamics of mobile ions with stable interface states, Phys. Rev. Appl. 17 (2022), 034042.
[5] S. Lin, X. Chen, Z.L. Wang, The tribovoltaic effect and electron transfer at a liquid-semiconductor interface, Nano Energy 76 (2020), 105070.
[6] Z.L. Wang, New wave power, Nature 542 (2017) 159–160.
[7] S.H. Kim, C.S. Haines, N. Li, K.J. Kim, K.J. Mun, C. Choi, J. Di, Y.J. Oh, J.P. Oviedo, J. Bykova, S. Fang, N. Jiang, Z. Liu, R. Wang, P. Kumar, R.;Priya Qiao, S. Cho, K. Kim, M. Lucas,M.S.;Drummy, L.F. Maruyama, B. Lee,D.Y, X. Lepro, E. Gao, D. Albarq, R. Ovalle-robles, S.J. Kim, R.H. Baughman, Harvesting electrical energy from carbon nanotube yarn twist, Science 357 (2017) 773–778.
[8] J. Falnes, A review of wave-energy extraction, Mar. Struct. 20 (2007) 185–201.
[9] Z. Wu, H. Guo, W. Ding, Y.C. Wang, L. Zhang, Z.L. Wang, A hybridized triboelectric-electromagnetic water wave energy harvester based on a magnetic sphere, ACS Nano 13 (2019) 2349–2356.
[10] S. Lin, X. Chen, Z. Wang, The tribovoltaic effect and electron transfer at a liquid-solid interface, Nano Energy 76 (2020), 105070.
[11] X. Liang, T. Jiang, G. Liu, T. Xiao, L. Xu, W. Li, F. Xi, C. Zhang, Z.L. Wang, Triboelectric nanogenerator networks integrated with power managementmodule for water wave energy harvesting, Adv. Funct. Mater. 29 (2019) 1807241.
[12] X. Liang, T. Jiang, Y. Feng, P. Lu, J. An, Z.L. Wang, Triboelectric nanogenerator network integrated with charge excitation circuit for effective water wave energy harvesting, Adv. Energy Mater. 10 (2020) 2002123.
[13] M. Zheng, S. Lin, L. Xu, L. Zhu, Z. Wang, Scanning probing of the tribovoltaic effect at the sliding interface of two semiconductors, Adv. Mater. 32 (2020) 2000928.
[14] C. Zhang, Z. Zhao, O. Yang, W. Yuan, L. Zhou, X. Yin, L. Liu, Y. Li, Z.L. Wang, J. Wang, Bionic-fin-structured triboelectric nanogenerators for undersea energy harvesting, Adv. Mater. Technol. 5 (2020) 2000531.
[15] Z. Zhao, Y. Dai, D. Liu, L. Zhou, S. Li, Z.L. Wang, J. Wang, Rationally patterned electrode of direct-current triboelectric nanogenerators for ultrahigh effective surface charge density, Nat. Commun. 11 (2020) 6186.
[16] L. Zhou, D. Liu, J. Wang, Z.L. Wang, Triboelectric nanogenerators: fundamental physics and potential applications, Friction 8 (2020) 481–506.
[17] J. Nie, Z. Wang, Z. Ren, S. Li, X. Chen, Z.L. Wang, Power generation from the interaction of a liquid droplet and a liquid membrane, Nat. Commun. 10 (2019) 2264.
[18] Y. Zi, H. Guo, Z. Wen, M.H. Yeh, C. Hu, Z.L. Wang, Harvesting low-frequency (<5 Hz) irregular mechanical energy: a possible killer application of triboelectric nanogenerator, ACS Nano 10 (2016) 4797–4805.
[19] X. Yang, J. Han, F. Wu, X. Rao, G. Zhou, C. Xu, P. Li, Q. Song, A novel retractable spring-like-electrode triboelectric nanogenerator with highly-effective energy harvesting and conversion for sensing road conditions, RSC Adv. 80 (2017) 50993–51000.
[20] Z.-H. Lin, G. Cheng, S. Lee, K.C. Pradel, Z.L. Wang, Harvesting water drop energy by a sequential contact-electrification and electrostatic-induction process, Adv. Mater. 26 (2014) 4690–4696.
[21] H. Wu, N. Mendel, D. van den Ende, G. Zhou, F. Mugele, Energy harvesting from drops impacting onto charged surfaces, Phys. Rev. Lett. 125 (2020), 078301.
[22] W. Xu, H. Zheng, Y. Liu, X. Zhou, C. Zhang, Y. Song, X. Deng, M. Leung, Z. Yang, R. X. Xu, Z.L. Wang, X. Zeng, Z. Wang, A droplet-based electricity generator with high instantaneous power density, Nature 578 (2020) 392–396.
[23] W. Xu, Z. Wang, Fusion of slippery interfaces and transistor-inspired architecture for water kinetic energy harvesting, Joule 4 (2020) 2523–2531.
[24] H. Gu, N. Zhang, Z. Zhou, S. Ye, W. Wang, W. Xu, H. Zheng, Y. Song, J. Jiao, Z. Wang, X. Zhou, A bulk effect liquid-solid generator with 3D electrodes for wave energy harvesting, Nano Energy 87 (2021), 106218.
[25] J. You, J. Shao, Y. He, F.F. Yun, K.W. See, Z.L. Wang, X.L. Wang, High-electrification performance and mechanism of a water−solid mode triboelectric nanogenerator, ACS Nano 15 (2021) 8706–8714.
[26] L. Pan, J. Wang, P. Wang, R. Gao, Y.-C. Wang, X. Zhang, J.-J. Zou, Z.L. Wang, Liquid-FEP-based u-tube triboelectric nanogenerator for harvesting water-wave energy, Nano Res 11 (2018) 4062–4073.
[27] S.L. Zhang, M. Xu, C. Zhang, Y.-C. Wang, H. Zou, X. He, Z. Wang, Z.L. Wang, Rationally designed sea snake structure based triboelectric nanogenerators for effectively and efficiently harvest- ing ocean wave energy with minimized water screening effect, Nano Energy 48 (2018) 421–429.
[28] H. Wu, N. Mendel, D. van den Ende, L. Shui, G. Zhou, F. Mugele, Charge trapping-based electricity generator (CTEG): an ultrarobust and high efficiency nanogenerator for energy harvesting from water droplets, Adv. Mater. 32 (2020) 2001699.
[29] L.E. Helseth, X.D. Guo, Fluorinated ethylene propylene thin film for water droplet energy harvesting, Renew. Energy 99 (2016) 845–851.
[30] H. Wu, Z. Wang, Y. Zi, Multi-mode water-tube-based triboelectric nanogenerator designed for low-frequency energy harvesting with ultrahigh volumetric charge density, Adv. Energy Mater. 11 (2021) 2100038.
[31] N. Zhang, H. Gu, K. Lu, S. Ye, W. Xu, H. Zheng, Y. Song, C. Liu, J. Jiao, Z. Wang, X. Zhou, A universal single electrode droplet-based electricity generator (SE-DEG) for water kinetic energy harvesting, Nano Energy 82 (2021), 105735.
[32] N. Zhang, H. Gu, H. Zheng, S. Ye, L. Kang, C. Huang, K. Lu, W. Xu, Q. Miao, Z. Wang, J. Zhang, X. Zhou, Boosting the output performance of volume effect electricity generator(VEEG) with water column, Nano Energy 73 (2020), 104748.
[33] L. Wang, Y. Song, W. Xu, W. Li, Y. Jin, S. Gao, S. Yang, C. Wu, S. Wang, Z. Wang, Harvesting energy from high-frequency impinging water droplets by a droplet-based electricity generator, EcoMat 3 (2021) 12116.
[34] Y. Chen, B. Xie, J. Long, Y. Kuang, X. Chen, M. Hou, J. Gao, S. Zhou, B. Fan, Y. He, Y. Zhang, C. Wong, Z. Wang, N. Zhao, Interfacial laser-induced graphene enabling high-performance liquid−solid triboelectric nanogenerator, Adv. Mater. 33 (2021) 2104290.
[35] H. Zhou, J. Dong, H. Liu, L. Zhu, C. Xu, X. He, S. Zhang, Q. Song, The coordination of displacement and conduction currents to boost the instantaneous power output of a water-tube triboelectric nanogenerator, Nano Energy 95 (2022), 107050.

[36] J. Dong, C. Xu, L. Zhu, X. Zhao, H. Zhou, H. Liu, G. Xu, G. Wang, G. Zhou, Q. Zeng, Q. Song, A high voltage direct current droplet-based electricity generator inspired by thunderbolts, Nano Energy 90 (2021), 106567.
[37] H. Wu, S. Wang, Z. Wang, Y. Zi, Achieving ultrahigh instantaneous power density of 10MW/m ^{2} by leveraging the opposite-charge-enhanced transistor-like triboelectric nanogenerator (OCT-TENG), Nat. Commun. 12 (2021) 5470.
[38] R.G. Neo, B.C. Khoo, Towards a larger scale energy harvesting from falling water droplets with an improved electrode configuration, Appl. Energy 285 (2021), 116428.
[39] X. Wei, Z. Zhao, C. Zhang, W. Yuan, Z. Wu, J. Wang, Z.L. Wang, All-weather droplet-based triboelectric nanogenerator for wave energy harvesting, ACS Nano 15 (2021) 13200–13208.
[40] X. Yang, S. Chan, L. Wang, W. Daoud, Water tank triboelectric nanogenerator for efficient harvesting of water wave energy over a broad frequency range, Nano Energy 44 (2018) 388–398.

Zong Li was born in Shandong province, China, on 4 September 1991. He received the B.S. in electrical engineering from Qingdao University, Qingdao, P.R. China, in 2016. He received the M.S. degrees in high voltage engineering from the Department of Electrical Engineering, Tsinghua University, Beijing, P.R. China, in 2019. His main research direction is TENG, high voltage external insulation and on-line monitoring technology.

Daiming Yang was born in Yulin, China, in 1990. He received the B.S. M.S. and Ph.D. degrees in electrical engineering from Tsinghua University, Beijing, China, in 2011, 2013 and 2019, respectively. He is currently a lecturer with Shenzhen Polytechnic School. His major research fields are high-voltage insulation, atmospheric corrosion, TENG, and battery energy storage.

Zhonghao Zhang was born in Shanxi Province, China, in May 1991. He received the B.S. degrees in power system and its automation from the Department of Electrical Engineering, North China Electric Power University, P.R. China, in 2013. He received the M.S. and Ph.D. degrees from the Department of Electrical Engineering, Tsinghua University, P.R. China, in 2016 and 2019, respectively. He is now working as AI algorithm engineer in China Electric Power Research Institute, Beijing, P. R. China. His research field is power intelligent operation and maintenance, state evaluation and fault diagnosis.

Dr. Shiquan Lin received his Ph.D. degree from Tsinghua University (THU) in 2018. he now works as a postdoctoral fellow under the supervision of Prof. Zhong Lin Wang in Beijing Institute of Nanoenergy and Nanosystems (BINN), Chinese Academy of Sciences. His research interests include fundamental tribological phenomena, scanning probe microscopy and frist-principle calculation.

Bin Cao was born in Shanxi province, China, in 1993. He received the B.S. in power system and its automation from North China Electric Power University in 2014. He received the M.S and Ph.D. degrees in high voltage engineering from the Department of Electrical Engineering, Tsinghua University, Beijing, China, in 2016 and 2019. He is now a postdoc at Graduate School at Shenzhen, Tsinghua University. His research field is outdoor insulation,TENG.

Liming Wang was born in Zhejiang province, China, on 30 November 1963, and received the B.S., M.S., and Ph.D. degrees in high voltage engineering from the Department of Electrical Engineering, Tsinghua University, Beijing, P.R. China, in 1987, 1990, and 1993, respectively. He has worked at Tsinghua University since 1993. His major research fields are high voltage insulation and electrical discharge, flashover mechanism on contaminated insulators,TENG, and application of pulsed electric fields.

Prof. Zhong Lin Wang received his Ph. D from Arizona State University in physics. He now is the Hightower Chair in Materials Science and Engineering, Regents' Professor, Engineering Distinguished Professor and Director, Center for Nanostructure Characterization, at Georgia Tech. Dr. Wang has made original and innovative contributions to the synthesis, discovery, characterization and understanding of fundamental physical properties of oxide nanobelts and nanowires, as well as applications of nanowires in energy sciences, electronics, optoelectronics and biological science. He pioneered the field of piezotronics and piezo-phototronics by introducing piezoelectric potential gated charge transport process in fabricating new electronic and optoelectronic devices.

Fanghui Yin was born in Jiangxi, China, in 1983. He received the B.S. and M.S. degrees from Chongqing University, Chongqing, China, in 2004 and 2008, respectively, and the Ph. D. degree from the Université du Québec à Chicoutimi (UQAC), Canada, in collaboration with Chongqing University, China. He currently holds an assistant professor position at the Graduate School at Shenzhen, Tsinghua University. His main research interests include high voltage technology, external insulation, and TENG.